CORA Cork Open Research Archive
Cartlann Taighde Oscailte Chorcaí

Title	Laser to laser power conversion with remote signaling
Authors	Roycroft, Brendan;Baskaran, Meena;McMahon, David;Corbett, Brian
Publication date	2021-05-24
Original Citation	Roycroft, B., Baskaran, M., McMahon, D. and Corbett, B. (2021) 'Laser to laser power conversion with remote signaling', Optics Express, 29(11), pp.16611-16618. doi: 10.1364/OE.423338
Type of publication	Article (peer-reviewed)
Link to publisher's version	10.1364/OE.423338
Rights	© 2021, Optical Society of America under the terms of the OSA Open Access Publishing Agreement.
Download date	2026-10-31 20:17:52
Item downloaded from	https://hdl.handle.net/10468/11407



UCC
University College Cork, Ireland
Coláiste na hOllscoile Corcaigh

Research Article | Vol. 29, No. 11 / 24 May 2021 / Optics Express 16611
Optics EXPRESS

Laser to laser power conversion with remote signaling

BRENDAN ROYCROFT,[1] MEENA BASKARAN,[1] DAVID MCMAHON,[2] AND BRIAN CORBETT[1,2,*]

[1]Tyndall National Institute, University College Cork, Cork, Ireland
[2]Physics Department, University College Cork, Cork, Ireland
[*]brian.corbett@tyndall.ie

Abstract: We demonstrate laser power conversion using an edge-coupled waveguide configuration. A laser with an emission energy of 0.87 eV (1427 nm) optically pumps a second with an emission energy of 0.80 eV (1540 nm), achieving the maximum possible open circuit voltage of 0.83 V due to optically pumped lasing. A fiber to device power conversion efficiency of 33% is achieved with internal power conversion efficiency ranging from 57% to 51%. The voltage at maximum power is 0.6 V, which is a record for the wavelength range. The same optically pumped device is used for effectively power-free 500 Mbps upstream data transmission, enabling compact powering and signaling for emerging applications in minimally invasive medical interventions and remote photonics.

© 2021 Optical Society of America under the terms of the OSA Open Access Publishing Agreement

1. Introduction

There are essential reasons for power delivery over optical fibres in settings where voltage isolation is necessary as well as for emerging opportunities in powering remote nodes in passive optical networks and in the Internet of Things [1–4]. In addition, minimally invasive endoscopic diagnostic medical interventions need highly compact components in order to investigate the smallest veins and ducts [5]. Miniature cameras with mm-sized cross-sectional dimensions are becoming available which will enable detailed tissue visualization during such procedures. These cameras need to be powered and to return high quality images through compact channels appropriate to the dimensions of single mode fibres [6].

Power transfer using light is maximised by providing monochromatic illumination at photon energies just above the bandgap of the receiving semiconductor photovoltaic (PV) cell. The state-of-the-art for laser power converters (LPC) using single-junction PV cells is 55% at 37 W/cm^2 [7] and 60% at 10 W/cm^2 [8]. In order to reduce the resistive losses at high currents, several photovoltaic cells are grown on each other with connecting tunnel junctions. Efficiencies of 50-60% were obtained with two junctions [9] and 65% for 5 junctions at a power density of 35 W/cm^2 [10]. These results were achieved at wavelengths around 800 nm using GaAs based cells. It is also desirable to operate in the 1300-1600 nm wavelength range to allow power delivery over longer distances using low-loss optical fibers. At 1550 nm, InGaAs cells have achieved a 43% efficiency at 0.1 W/cm^2 [11] while GaSb cells achieved a 43% power conversion at 20 W/cm^2 [12].

Key to the performance of the PV cell is maximising the open circuit voltage, V_{oc}, which is determined by the generated carrier concentrations [13] with $V_{oc} = kT/q \ln(np/n_i^2)$, where n, p are the electron and hole concentrations, n_i, is the intrinsic carrier concentration, k, the Boltzmann constant and T, the temperature. Thus, high V_{oc} requires the use of high incident optical power densities to create high carrier densities. Typically, a maximum open circuit voltage of 1.20 V is obtained for GaAs cells which has a bandgap of 1.41 V. However, such cells are limited at increasing power density by resistive and thermal effects resulting in a severe reduction in the fill factor. The maximum power densities are 20-50 W/cm^2 equivalent to 200-500 suns. This

#423338 https://doi.org/10.1364/OE.423338
Journal © 2021 Received 1 Mar 2021; revised 30 Apr 2021; accepted 4 May 2021; published 14 May 2021

Optics EXPRESS

concentration range is used in achieving record performance in solar cells where the current record of 46% was measured at 508 suns for a 4-junction device [14]. An InGaAs solar cell (under broadband illumination) has a V_{oc} of 0.46 V under 560 suns [15]. The reported LPCs are configured to collect light incident from a surface normal direction as used in conventional PV cells (Fig. 1(a)). A high density of conductive grid connections are necessary in order to collect the current with minimised resistance at high optical concentrations. The required grid density increases with operational current leading to a significant shadowing of the incident light. Such arrangements are compatible with light sources of large cross sectional area operating at a low current density and consequently low carrier density.

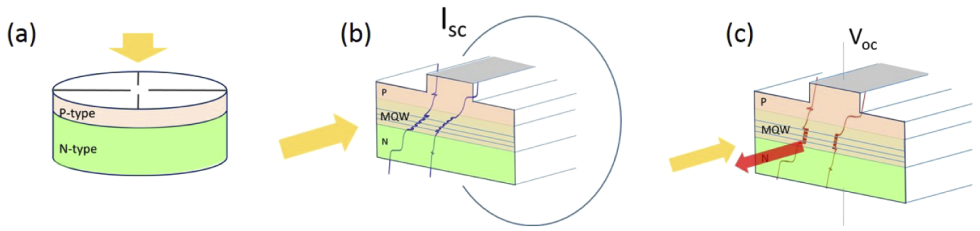


Fig. 1. Structure and design of the LPC. (a) Conventional surface-normal coupling of light into an absorber with a p-n doped junction, (b) edge coupling geometry to a multiple quantum well absorbing region at short circuit conditions with efficient carrier extraction, (c) edge coupling geometry at open circuit conditions. At sufficient input optical power, the LPC is driven to lasing resulting in an open circuit voltage in excess of the bandgap of the quantum wells.

In this paper, we explore edge-coupling between two fiber-coupled waveguided lasers at telecom wavelengths and show that this geometry enables record overall power conversion efficiency in a highly compact footprint. We demonstrate that it is possible to optically pump the receiving device to lasing and that, as a result, the maximum possible open circuit voltage for a single-junction PV cell is achieved. The same remotely powered device is modulated at open circuit to effect high speed data transfer with minimal power demand from the distal end.

2. Concept

Using thermodynamic arguments it has been shown that the highest efficiency solar cells correspond to the most efficient LEDs [16]. Thus, we can expect that that the highest performing LPCs also correspond to the best lasers [17]. Here, we edge couple the laser light to the PV cell which itself is a waveguided quantum well (QW) based laser (Fig. 1(b), (c)). In this case, the direction of carrier transport is perpendicular to the direction of the input light allowing advantages of (1) no blocking of the light by the electrical contacts, (2) absorption of light in thin QWs enabling high carrier density and thus high open circuit voltage, (3) direct generation of carriers in the thin p-n junction region resulting in strong electric field for carrier separation, (4) short distance for the transport of the charges with no resistance contributions associated with lateral carrier transport where conventional cells rely on the transport of minority carriers to the opposite sides of the junction, (5) reduced radiative recombination due to reduced volume of absorbing material, and (6) applicable to wide wavelength range due to availability of high performance semiconductor lasers.

Optical injection is a well-known technique for controlling the properties of edge-emitting semiconductor lasers such as wavelength locking or inducing various dynamics. In those cases, the wavelength of the injected light is close to the laser wavelength. Optical power conversion for microwave signal generation is also widely used with waveguide photodetectors. There, the devices are operated in reverse bias and with short device lengths in order to achieve high

Optics EXPRESS

bandwidths. While edge-coupling is commonly used to pump fiber lasers we are not aware of previous reports of optically pumping a semiconductor laser to lasing by using edge-coupling.

3. Experiment and results

We used two commercially obtained lasers, transmitter and receiver (the LPC), each coupled to standard single-mode optical fiber. The transmitting laser is a fiber Bragg grating stabilised laser (Alcatel-Fitel) emitting at a wavelength of 1.43 μm (0.87 eV) while the receiving Fabry-Perot laser (Thor Labs FPL1009S) emits at a wavelength of 1.54 μm (0.80 eV) with a threshold current of ~35 mA corresponding to 1.2 kA/cm^2 assuming a waveguide width of 3 μm, and a fiber coupled efficiency of 0.24 W/A. Thus, the thermalisation loss (Stokes shift) in the receiver is 70 meV. A cavity length of 1 mm is estimated for the LPC from the separation of the individual Fabry-Perot modes in its emission spectrum. The series resistance of the LPC is 1.6 Ω. The lasers are directly joined through the attached single mode fibres without an optical isolator. By using the receiving laser as a photodetector the coupling efficiency from the transmitting laser to the receiving waveguide is 65 ± 1%. The loss is due to the fiber connection, the lens coupling and the coating on the front facet of the receiving laser. The absorption of edge-illuminated quantum wells is polarization sensitive at wavelengths around the bandgap. Using a tuneable laser and polarisation rotation, we measured the TE and TM polarized absorption of the receiving laser and confirmed enhanced TE absorption at the bandgap corresponding to compressively strained wells. However, the absorption is polarization independent for incident wavelengths less than 1450 nm as is the case here.

The current – voltage (I-V) characteristics of the LPC under optical pumping are shown (Fig. 2(a)) as a function of absorbed power up to 80 mW. The absorbed power is calculated from the reverse current at -1 V using the bandgap responsivity. Figure 2(b) shows the evolution of the short circuit current, I_{sc}, with absorbed power. At low powers, all the carriers are collected at I_{sc} as there is no further increase with a reverse bias of -1 V. At the highest powers while the absorption is not saturated, not all of the carriers are collected at I_{sc} due to the screening of the electric field by the generated charge in the QWs. A loss of 5% in I_{sc} is measured for an absorbed power of 80 mW. This corresponds to a delivered power density of $> 10^6$ W/cm^2, equivalent to $> 10^7$ suns, assuming a transverse mode width of 1.5 μm. Such power densities are orders of magnitude larger than used with current laser power converters or in concentrator solar cells but are normal in the context of lasers. The typical carrier density for lasing threshold in quantum wells at this wavelength is n, p ~ 2×10^{18} cm^{-3} and is reached under optical injection in our experiment. At the highest power used the short circuit current is 93 mA which, if absorbed along the entire length of the waveguide corresponds to a current density of 3.1 kA/cm^2.

An absorption length (63% absorption) of 25 μm is estimated which is much shorter than the 1 mm length of the waveguide. This is based on an absorption coefficient of 8,000 cm^{-1} for the QWs at the incident wavelength and a mode overlap of 5% as is typical for a waveguide containing a few QWs. Even with a single QW, the estimated absorption length is only 125 μm. However, in the LPC, the positive voltage locally generated due to absorption of carriers is re-distributed along the length of the waveguide through the low resistance metal contacts resulting in turn of a re-distribution of the carriers along the entire length of the device [18,19]. The associated response time is set by the Resistance*Capacitance constant of the device. The energy is deposited directly in the QWs due to the small 70 meV offset in energy between the pump and absorption. The 70 meV results in little change in the polarization independent absorption that would be affected by carrier screening for pumping closer to the bandgap energy. Restricting absorption to the QW prevents excess local absorption in the facet region which would lead to current crowding affecting voltage redistribution and potential facet damage. The fact that lasing is reached is evident that screening is not a dominant issue. Our assessment is that a single QW is the ideal absorber as it increases the absorption length, allows reduction

Optics EXPRESS

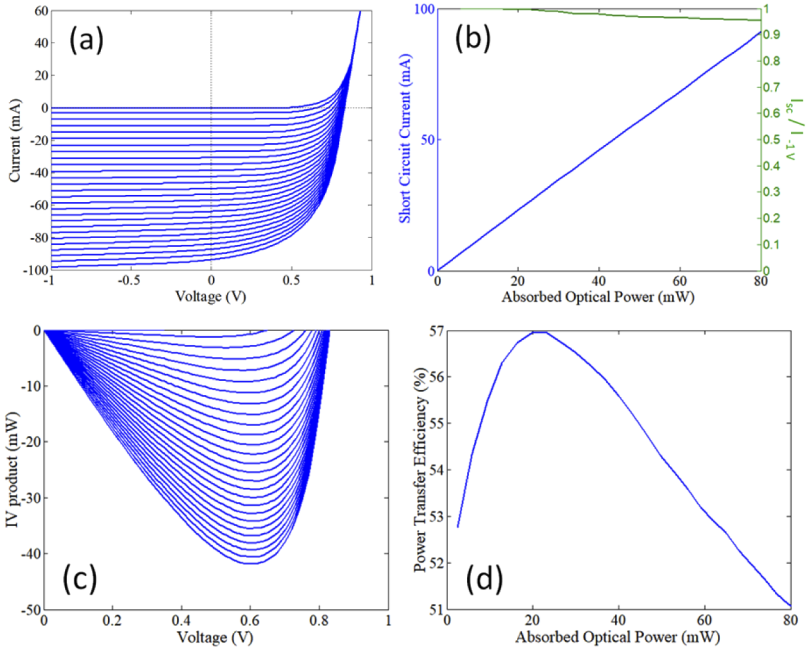


Fig. 2. Characteristics of laser power converter as a function of absorbed power. Optical power between 0 and 80 mW absorbed in steps of 3.08 mW with the LPC held at 20°C. (a) I-V characteristics, (b) Short circuit current with absorbed power (left axis). Collected current at short circuit compared with that at -1 V showing slight saturation of Isc at highest absorbed power (Right axis). (c) Power conversion vs voltage. (d) Internal power transfer efficiency vs. absorbed power.

in the undoped region for a higher inbuilt electric field and enables non-trapping transport for collection of the electrons and holes.

Figure 2(c) shows the power generated as function of output voltage. The power transfer efficiency (PTE) is calculated from maximum electrical power from the receiving laser divided by the power absorbed by the laser. The voltage at the maximum power point, V_{mpp}, is 0.6 V which is a record for this wavelength. Figure 2(d) shows that the maximum PTE achieved is 57% for an absorbed power of 20 mW. An electrical power of 42 mW is obtained for an absorbed optical power of 80 mW corresponding to a PTE of 51%. The fill factor reaches 68% at low incident power and drops to 54% at an absorbed power of 80 mW. This reduction is due to charge screening limiting carrier escape for voltages < 0.75 V where carrier density is estimated to be 5×10^{17} cm^{-3}. At higher carrier densities Auger recombination is significant for 1550 nm lasers and can account for up 55% of all recombination at threshold [20].

With increasing pump powers V_{oc} increases (Fig. 2(a)) due to the high carrier density achieved in the QWs until clamping of V_{oc} at 0.83 V for absorbed powers > 45 mW. At V_{oc}, no power is extracted through the contacts and the energy is dissipated by radiative recombination (spontaneous emission and lasing), non-radiative Auger recombination in addition to heat generated by thermalisation of the pump photons. When V_{oc} is 0.83 V the LPC is lasing with the quasi-Fermi level splitting being greater than the energy of the emitted laser light and also greater than the bandgap of the MQW according to the Bernard-Duraffourg condition [21]. The dynamic resistance, R_{dyn}, scales as 1/I until the lasing threshold is reached at which point a strong kink is obtained and the resistance drops to the series resistance of the laser [22]. The extracted laser threshold is shown in Fig. 3(a) as a function of absorbed power where it decreases linearly with

Optics EXPRESS

pump power at a rate of 0.7 mA/mW or 0.61 mA/mA of absorbed current corresponding to the subthreshold injection efficiency of the laser [23]. The threshold current becomes negative for absorbed powers > 45 mW. V_{oc} is clamped at 0.83 V for pump powers that exceed the threshold. At voltages just below V_{oc} part of the charge generated in the LPC is collected as reverse current and voltage, while part of the absorbed power is re-emitted as laser light reducing the collected current. Figure 3(b) shows the spectrum of the LPC in lasing mode along with the pump laser spectrum reflected from the LPC facet collected with the aid of a circulator while Fig. 3(c) shows the evolution of the LPC to lasing under optical pumping. Figure 3(d) shows a close-up of the individual modes and their evolution with pump power. The Fabry-Perot modes initially blue shift with increasing pump power due to a decrease in the refractive index. This is due to increasing carrier density which results in plasma dispersion, band filling, bandgap renormalisation and gain-index coupling. As the pump power increases the modes then red shift indicating heating of the waveguide. The change in refractive index for a quaternary layer with a bandgap wavelength of 1.15 μm at 1.55 μm with temperature, $\Delta n/\Delta T$, is 0.26×10^{-3} K^{-1} which indicates that the temperature of the active region increases by 2 K.

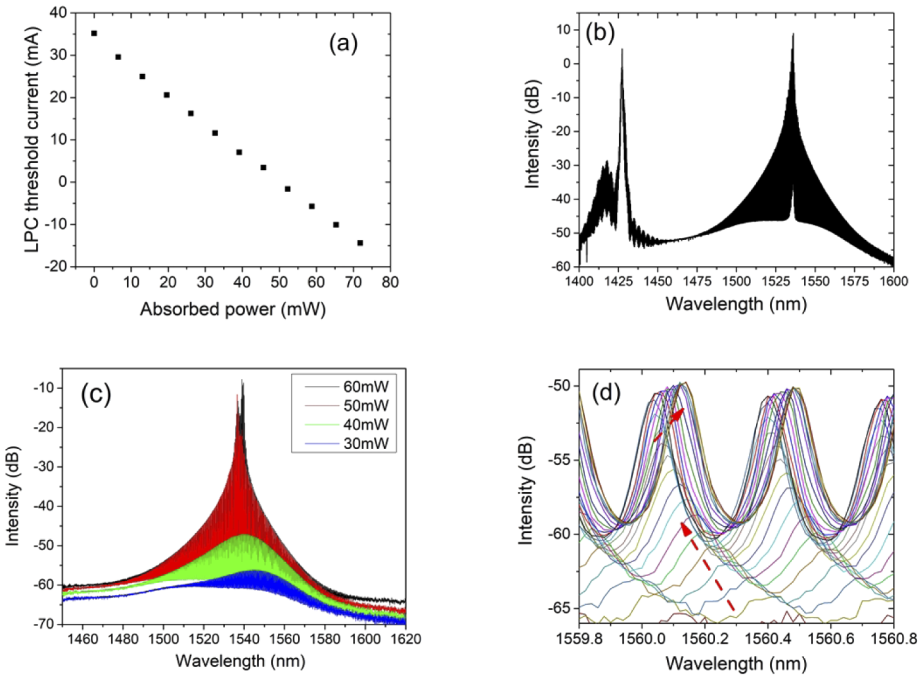


Fig. 3. Lasing characteristics of LPC. (a) Threshold current of the LPC under optical pumping extracted from the dynamic resistance. At absorbed optical powers above 45 mW the LPC lases with no electrical bias and current can be drawn from the LPC while lasing, (b) Lasing spectrum from LPC along with reflected pump light, (c) Emission spectra from the LPC under increasing absorbed optical powers (30, 40, 50 and 60 mW) provided from the transmitter, (d) Evolution of the individual optical modes of the LPC under pumping showing an initial shift to shorter wavelengths due to increasing carrier densities, followed by a shift to longer wavelengths once the device lases due to carrier clamping and thermal effects.

The LPC is configured to transmit optical data in the upstream direction when being optically pumped. A 2^9-1 pseudo random bit sequence (PRBS9) data signal is applied from a pulse pattern generator (PPG) to the LPC delivering a small ac voltage (measured as 22 mV_{pp} delivered to the laser) at bit rates from 100 Mbps to 500 Mbps. The signal is detected, with the aid

Optics EXPRESS

of a circulator, on a 1 GHz bandwidth photoreceiver and displayed on an 8 GHz bandwidth oscilloscope (Fig. 4(a)). To avoid DC shunting of the LPC due to the 50 Ω impedance of the PPG, a DC block is inserted. The laser operates around zero current with the voltage being modulated around Voc. Figure 4(b) shows the received signal for different pump powers where the device is being modulated with a measured modulation voltage of ±11 mV and modulation current of ±6 mA. Figure 4(c) inset shows the received eye diagrams at 100 and 500 Mbps. At 100 Mbps, the bit error rate (BER) is estimated from the measured Q-factor to be approximately 10^{-11}, and is $\sim 10^{-4}$ at 500 Mbps which can be made error free by forward error correction. As the LPC is externally optically pumped to lasing, the positive 11 mV swing of the pulse generator is not necessary in order to achieve signaling - the LPC only needs to be shunted below threshold as the shunt current removes carriers from the QWs and turns off the laser. In other words, as the LPC is already optically pumped to lasing, no power needs to be supplied to the LPC by the pattern generator. Specifically, the modulated current swing is 12 mA, and from Fig. 3(a) the open circuit device is 12 mA above threshold when optically pumped with 65 mW absorbed power. Hence, if the device is switched between open and short circuit with the pump laser emitting 140 mW, to take into account the circulator and coupling loss to the receive laser, the amplitude of the transmitted data signal will be the same as that when using the pattern generator. When the LPC is not lasing, the shunted current can be used to electrically charge an on-board capacitor, and when the device is lasing, it does not require any electrical power from that capacitor as it is already optically pumped to lasing. Thus, the same device can act both as a compact remote

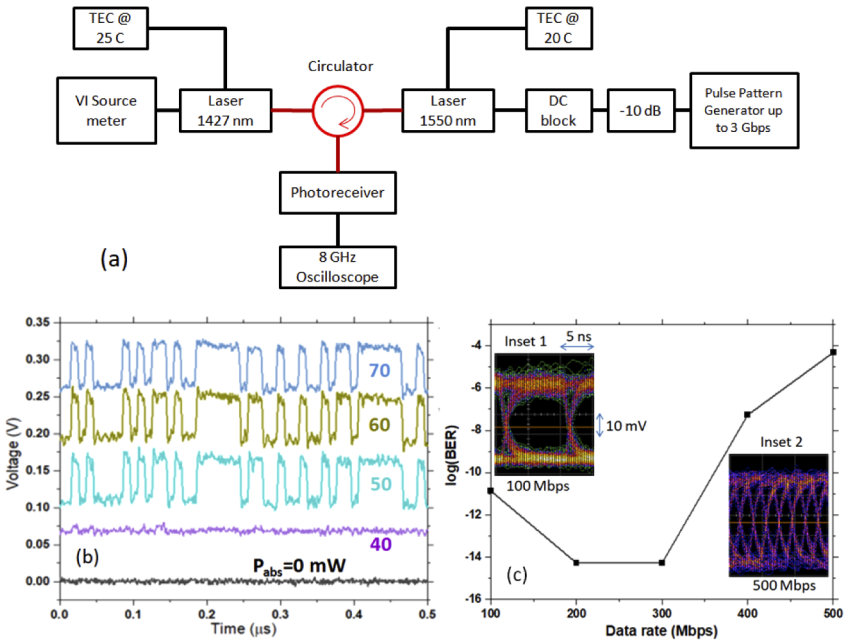


Fig. 4. Data transmission with LPC. (a) Experimental setup, electrical connections denoted with black lines, optical connections with red. (b) Received data stream as the optical pump power is increased. Black: no optical pump power, Magenta: incident 40 mW absorbed optical pump power, which is insufficient for lasing, light blue = 50 mW absorbed optical pump power where the downstream detector is above threshold, green: 60 mW, blue: 70 mW. Vertical axis is voltage of the upstream photoreceiver, (b) BER estimated from the Q factor measured by the oscilloscope for each data rate at 60 mW optical pump power. Inset 1: eye diagram at 100 Mbps, Inset 2: 500 Mbps.

Optics EXPRESS

power converting element and as a remote high speed signaling device. As the LPC is pumped to lasing, the internal bandwidth limitation should be in the GHz range and in this case the bandwidth is limited by the RC time constant of the 14-pin butterfly package.

4. Conclusion

We have introduced a new strategy to achieve efficient optical power conversion in a highly compact format. Record performance is achieved reaching the maximum achievable V_{oc} of 0.83 V, a V_{mpp} of 0.6 V, internal conversion efficiency 57% and effectively power-free upstream data signalling to 500 Mbps. Routes to further improve performance are to increase carrier extraction through band-structure engineering [24] and to use wavelengths around 900 nm where the most efficient semiconductor lasers operate. The use of a laser as the photovoltaic element fulfils some essential requirements towards the ultimate efficiency of an optical power converter based on a reversible emitter-absorber system. Namely, an extremely high luminescence efficiency and matching the etendu between the emitter and absorber which can only be achieved by lasers [17]. This approach opens new opportunities for LPCs arising with the increasing deployment of single mode optical fibers in data centres, signalling to the home and in the Internet of Things.

Funding. Science Foundation Ireland (12/RC/2276_P2, 19/US-C2C/3579).

Disclosures. BC and BR: University College Cork (P).

Data availability. Data underlying the results presented in this paper may be obtained from the authors upon reasonable request.

References

1. J-G. Werthen, "Powering Next Generation Networks by Laser Light over Fiber," OFC/NFOEC 2008 Paper OWO3 (2008).
2. M. Roger, G. Bottger, M. Dreschmann, C. Klamouris, M. Huebner, A. W. Bett, J. Becker, W. Freude, and J. Leuthold, "Optically powered fiber networks," Opt. Express **16**(26), 21821–21834 (2008).
3. J. D. López-Cardona, D. S. Montero, and C. Vázquez, "Smart Remote Nodes Fed by Power over Fiber in Internet of Things Applications," IEEE Sensors J. **19**(17), 7328–7334 (2019).
4. M. Matsuura, N. Tajima, H. Nomoto, and D. Kamiyama, "150-W Power-Over-Fiber Using Double-Clad Fibers," J. Lightwave Technol. **38**(2), 401–408 (2020).
5. M. J. Mack, "Minimally Invasive and Robotic Surgery," J. Am. Med. Assoc. **285**(5), 568–572 (2001).
6. M. Peka, J. van Rens, and M. B. van der Mark, "Electrifying catheters with light," Opt. Express **25**(8), 8534–8549 (2017).
7. E. Oliva, F. Dimroth, and A. W. Bett, "GaAs converters for high power densities of laser illumination," Prog. Photovolt: Res. Appl. **16**(4), 289–295 (2008).
8. V. P. Khvostikov, N. A. Kalyuzhnyy, S. A. Mintairov, S. V. Sorokina, N. S. Potapovich, V. M. Emelyanov, N.Kh Timoshina, and V. M. Andreev, "Photovoltaic laser-power converter based on AlGaAs/GaAs heterostructures," Semiconductors **50**(9), 1220–1224 (2016).
9. J. Schubert, E. Oliva, F. Dimroth, W. Guter, R. Loeckenhoff, and A. W. Bett, "High-Voltage GaAs Photovoltaic Laser Power Converters," IEEE Trans. Electron Devices **56**(2), 170–175 (2009).
10. S. Fafard, M. C. A. York, F. Proulx, C. E. Valdivia, M. M. Wilkins, R. Arès, V. Aimez, K. Hinzer, and D. P. Masson, "Ultrahigh efficiencies in vertical epitaxial heterostructure architectures," Appl. Phys. Lett. **108**(7), 071101 (2016).
11. S. D. Jarvis, J. Mukherjee, M. Perren, and S. J. Sweeney, "Development and characterisation of laser power converters for optical power transfer applications," IET Optoelectron. **8**(2), 64–70 (2014).
12. V. P. Khvostikov, S. V. Sorokina, O. A. Khvostikova, N. S. Potapovich, A.V. Malevskaya, M. V. Nakhimovich, and M. Z. Shvarts, "GaSb photovoltaic cells for laser power conversion," AIP Conf. Proc. **2149**, 050007 (2019).
13. R. R. King, D. Bhusari, A. Boca, D. Larrabee, X. Q. Liu, W. Hong, C. M. Fetzer, D. C. Law, and N. H. Karam, "Band gap-voltage offset and energy production in next-generation multijunction solar cells," Prog. Photovolt: Res. Appl. **19**(7), 797–812 (2011).
14. M. A. Green, Y. Hishikawa, W. Warta, E. D. Dunlop, D. H. Levi, J. Hohl-Ebinger, and A. W. H. Ho-Baillie, "Solar cell efficiency tables (version 50)," Prog. Photovolt. Res. Appl. **25**(7), 668–676 (2017).
15. M. P. Lumb, M. Meitl, I. W. Wilson, S. Bonafede, S. Burroughs, D. V. Forbes, C. G. Bailey, N. M. Hoven, M. Gonzalez, M. K. Yakes, S. J. Polly, S. M. Hubbard, and R. I. Walters, "Development of InGaAs Solar Cells for >44% Efficient Transfer-Printed Multi-junctions," *IEEE 40th Photovoltaic Specialist Conference (PVSC)* 0491–0494, (2014).
16. O. D. Miller, E. Yablonovitch, and S. R. Kurtz, "Strong internal and external luminescence as solar cells approach the Shockley-Queisser limit," IEEE J. Photovoltaics **2**(3), 303–311 (2012).

Optics EXPRESS

17. M. A. Green, "Limiting photovoltaic monochromatic light conversion efficiency," Prog. Photovolt. Res. Appl. **9**(4), 257–261 (2001).
18. G. Livescu, D. A. B. Miller, T. Sizer, D. J. Burrows, J. E. Cunningham, A. C. Gossard, and J. H. English, "High-speed absorption recovery in quantum well diodes by diffusive electrical conduction," Appl. Phys. Lett. **54**(8), 748–750 (1989).
19. S. Presa, P. P. Maaskant, M. J. Kappers, and B. Corbett, "Fluorescence microscopy investigation of InGaN-based light-emitting diodes," IET Optoelectron. **10**(2), 39–43 (2016).
20. S. Sweeney, D. McConville, S. R. Jin, C.N. Ahmad, N. F. Masse, R. X. Bouyssou, A. A. Adams, and C. Hanke, "Temperature and wavelength dependence of recombination processes in 1.5 μm InGaAlAs/InP-based lasers," *16th International Conference on Indium Phosphide and Related Materials*, Kagoshima, Japan 738–741 (2004).
21. M. G. A. Bernard and G. Duraffourg, "Laser conditions in semiconductors," Phys. Status Solidi B **1**(7), 699–703 (1961).
22. S. Weisser, I. Esquivias, P. J. Tasker, J. D. Ralston, B. Romero, and J. Rosenzweig, "Impedance characteristics of quantum-well lasers," IEEE Photonics Technol. Lett. **6**(12), 1421–1423 (1994).
23. P. M. Smowton and P. Blood, "The differential efficiency of quantum-well lasers," IEEE J. Sel. Top. Quantum Electron. **3**(2), 491–498 (1997).
24. Y. Wen, Y. Wang, K. Watanabe, M. Sugiyama, and Y. Nakano, "Enhanced Carrier Escape in MSQW Solar Cell and Its Impact on Photovoltaics Performance," IEEE J. Photovoltaics **2**(2), 221–226 (2012).

143.239.102.69 {ts '2021-05-28 08:40:16'}